Revista Internacional de Investigación e Innovación Tecnológica

Página principal: www.riiit.com.mx

Design and construction of a compact low-cost test bench for hybrid engine studies

Diseño y construcción de un banco de pruebas compacto y económico para estudios de motores híbridos

Trejo-Mandujano, H.[a], Mejía-Cisneros. G.[b], Ordoñez-Casanova, E.[b]

[a] Department of Physics and Mathematics, Universidad Autónoma de Ciudad Juárez.
[b] Department of Industrial Engineering and Manufacturing, Universidad Autónoma de Ciudad Juárez; Av. Plutarco Elías Calles 1210, Fovissste Chamizal, Ciudad Juárez, Chihuahua, México.
htrejo@uacj.mx; guillermo.mejia@uacj.mx; eordonez@uacj.mx

Technological innovation: Utility model for data acquisition in the investigation of the conversion of internal or conventional combustion engines to hybrids.

Industrial application area: Mexican automotive industry.

Received: april 29th, 2021
Accepted: december 13th, 2021

Resumen

En este artículo se presenta el diseño, la construcción y los primeros resultados de un banco de pruebas de motores híbridos de bajo costo. El propósito de este dispositivo es permitir una investigación geográficamente específica, sobre algoritmos de control y arquitecturas en torno a vehículos de propulsión híbrida. El sistema consta de un motor de combustión interna acoplado en serie-paralelo a un motor eléctrico de corriente continua capaces de suministrar propulsión de forma independiente o conjugada a una carga inercial. El dispositivo incluye un circuito de gestión que utiliza sensores, actuadores, pantallas y dispositivos de memoria alrededor de un microcontrolador para controlar la entrega de energía, adquirir información, mostrar y guardar los datos necesarios para la investigación. Con este dispositivo relativamente económico, se pretende hacer varias pruebas bajo diferentes condiciones y así inferir el costo/beneficio de convertir un vehículo de combustión interna original a híbrido donde se consideren las necesidades de transporte específicas de cada ciudad. Como resultados se muestran el diseño mecánico y electrónico, así como las adquisiciones de las primeras pruebas experimentales como prueba del concepto.

Palabras claves: Motores híbridos, banco de pruebas, instrumentación.

Abstract

In this paper, the design, construction and first results of a low-cost hybrid engine test bench is presented. The purpose of this device is to allow geographically specific research around control algorithms and architectures for hybrid engines. The system consists of an internal combustion engine parallel-coupled to a direct current electrical motor, which can independently supply power to an inertial load. The device includes a management circuit that uses sensors, actuators, displays and memory devices around a micro-controller to control power delivery, acquire information, display, and save data needed for the investigation. The general objective of this low-cost device is to make several tests under different conditions to infer the cost/benefit of converting an original internal combustion powered vehicle into a hybrid, considering the city specific transportation needs. As results, the mechanical and electronic design are shown the data acquisition as well of first experimental tests as proof of concept.

Keywords: Hybrid Engines, Test Bench, Instrumentation.

1. Introduction

A partial and slow solution to the pollution and fossil fuel dependency problem generated by passenger cars is through the introduction of electric or hybrid cars by manufacturers [1–6]. This approach involves a high initial cost for the buyer, still low autonomy, and batteries lifetime. Even that the mentioned disadvantages were improved, we are dealing with a replacement technology, i.e., it does not account for the millions of cars operating by internal combustion engines (ICE) that are currently on the roads. In other words, hybrid or electric is not an add-on technology as the end-user need to completely replace his ICE vehicle for a hybrid or electric car. Although this is common on the developed world, in countries under development, the replacement scheme would imply a long delay in the introduction of the new technology. For example, table 1 show that in 2018 the hybrid sales in Mexico accounted for only 2% of the total sales.

Table 1. Statistical information provided by México's National Institute of Statistics and Geography (INEGI) for ICE and hybrid cars in 2018 [7, 8].

Concept	Quantity
Registered in circulation in Mexico	31534604
Registered in Chihuahua state	1123460
Car sales in Mexico	858525
Hybrid sales in Mexico	17600
Hybrid sales in Chihuahua state	197

Also, the research of electric and hybrid cars can be divided mostly around energy storage [9,10], system power [11,12], energy control and management [13–15], energy production and recovery [16–18] and/or systems architecture [19–21], leaving the investigation for engine conversion outside the research mainstream.

Moreover, those investigations rarely account for the geographical conditions like weather and/or driving aspects in a city, among others. For instance, they might be regions that have good climate 300 days of the year, flat geography at sea level and other regions with constant wind and roller coaster type roads at 1120 m above sea level. Accounting for those parameters might result in higher efficiency of converting vehicles under the specific environmental conditions.

These circumstances encourage to make geographic-specific research on the feasibility and efficiency of converting current ICE cars into hybrids. To promote such research, building a test bench that can be constructed with readily available parts is desirable. Some authors have undertaken this idea in different ways. For instance, in [22], they build a test bench comprised of a diesel engine, 2 permanent magnet synchronous electric motors and extra electric motor to simulate resistance. This setup allows to study hybrid engines in parallel and series with different degrees of hybridization.

Although the setup is very complete, it utilizes very specialized and expensive equipment. Another test bench is explained in [23] with the aim of making research on purely electric cars operated by a lithium-iron phosphate batteries and fuel cells. It includes an electric dynamometer with the scope of studying those power sources under different operation conditions. Finally, on [24] a model chassis powered by an electric motor (ME) and ICE in series, parallel or both is found. They employ low-cost components to show how the diverse architectures and components operates and interact, but only for demonstration purposes.

Considering the above, the design and construction of a test bench is shown in this paper. The purpose is to allow for researchers, technologist, and engineers to explore the regional optimal parameters and algorithms, to efficiently adapt or convert their commonly used ICE vehicles into electric or hybrid. Because the target is the developing countries, the present design is compact, low-cost, and constructed with materials that are readily available. In the following sections, the general layout and mechanics of the device are displayed. After that, the electronic part of the system is presented, then the general operation and finally the first results of the device are shown as proof of concept.

2. The Mechanical System

The base of the system consists of a recycled bicycle frame mounted on a stand. The setup holds the ICE, the direct current electric motor (DCEM), fuel deposit, battery bank, sensors, actuators, inertial and friction load and all the mechanical linkage needed as shown in figure 1. The reason to use a recycled bicycle comes from the convenience that it already holds the bearings that carries gears as well the necessary mountings for the inertia load in place of the rear wheel. These frames are easily obtainable almost everywhere having the extra benefit of reusing disposed bicycles. The whole system can be fixed on tabletop to make it ergonomically accessible.

2.1. Mechanical Power

The mechanical power introduced to the load comes from an 80 cc two-stroke ICE, and a 1000Watt DCEM. Our device retains its original pedals (P in figure 2) which allows human provided power in case the user want to investigate a 3-power source hybrid. All the power sources parallel their outputs, energy through multiple gears to an also several geared loads using chains (See figure 2). This arrangement allows to choose multiple combinations of gear ratios. Additionally, all the gears in the power sources are of the ratchet type (it locks in one direction and freewheel on the other) to apply power to the load independently and to assure that no power source drags another.

2.2. Fuel deposit.

The fuel deposit can be any fuel safe container with a hose connected from the bottom and into the ICE. It is desirable that the main fuel deposit sits higher than the ICE to eliminate the need of a fuel pump (figure 1). For our case, the deposit is a recycled small motorcycle fuel tank. At the tank output, a control valve was included and from there the fuel passes into a T-connector that splits the fuel into the ICE and into the fuel level sensor.

2.3. The load

To measure the power produced by the 3 sources, it needs to be applied to some type of

load. For this apparatus, an inertia load was selected which consists of a balanced rotational device with known moment of inertia about the rotation axis. This simple setup allows for torque measurement under acceleration as in an inertia dynamometer [25-27]. A big enough moment of inertia is desirable for two reasons: to accurately simulate the mass of the vehicle and to experiment with energy recovery from the load to the batteries. The mass equivalent of a vehicle under acceleration can be calculated trough energy considerations:

$$\frac{1}{2}mv^2 = \frac{1}{2}I\omega^2 \qquad \textbf{(Eq. 1)}$$

Considering a wheel of radius r then the no slip velocity is $v = r\omega$ therefore can be solved for m:

$$m = \frac{I}{r^2} \qquad \textbf{(Eq. 2)}$$

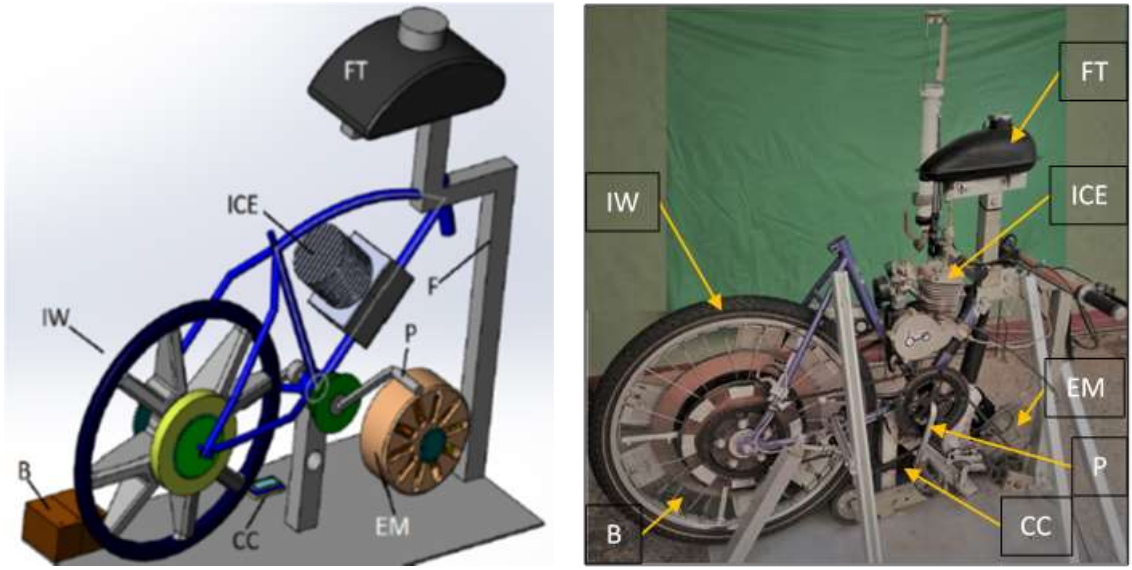

Figure 1. The general layout of the devices consists of a stand that supports a bicycle frame (F)that holds the fuel tank (FT), combustion engine (ICE), electric motor (EM), inertia wheel (IW), pedals (P), batteries (B) electronics and control circuit (CC).

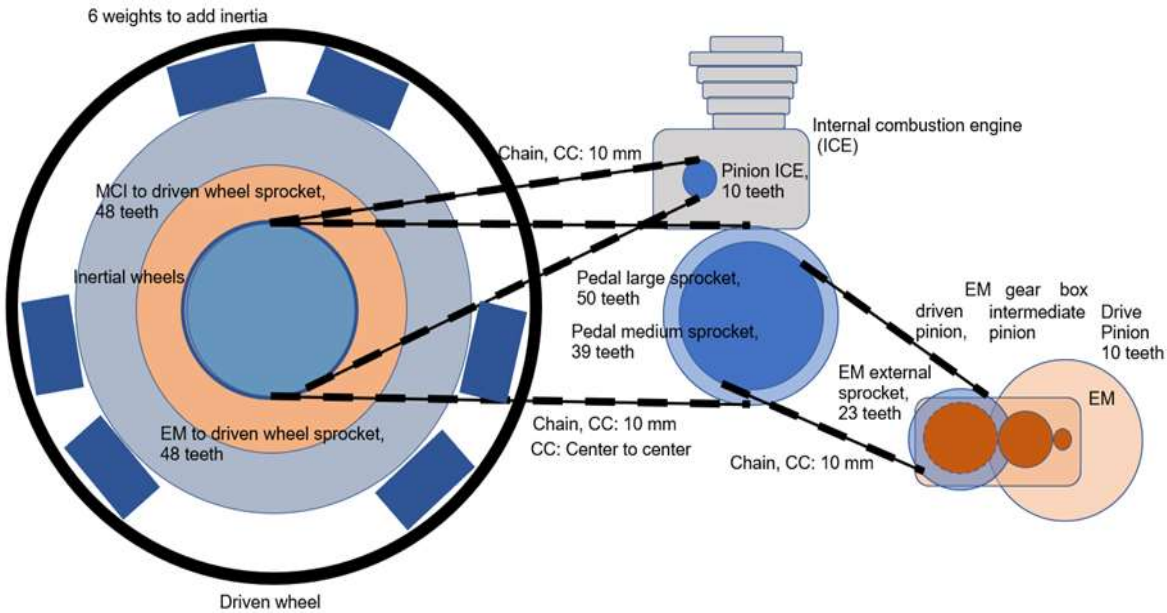

Figure 2. The diagram shows how the mechanical power is parallel transmitted to the load. Observe that the DCEM couples to the load through the pedal's gears.

The original bicycle rear wheel was used in which a concentrically weight plate was added. Also, several weights like the used to balance care tires were added at the rim edge to balance the system and to increase the moment of inertia (figure 3). The final assembly of the load was computer rendered and the moment of inertia calculated using finite element software. Additionally, a friction device is included that consists of a free wheel pressing into the inertia wheel. For now, this device can only be set to a constant pressure drag for each run; this approach permits for dynamical power measurements only, thus it cannot acquire variable load power data at constant revolutions per minute (RPM). In a future revision, a variable electronic controlled friction device will be introduced.

3. Electronic display, acquisition, and control

The data acquisition and control system of the test bench consist of sensors, actuators, displays, and a data storage device around the Atmel 328P micro-controller in the Arduino UNO R3 platform. Most of these peripherals where in module form and can be acquired from China suppliers at very low-cost and shipped worldwide. Using prefabricated modules instead of building the complete peripheral (composed of the sensor, amplifiers, filters, voltage regulator, etc.) is more cost-effective at China suppliers' prices.

3.1. Printed Circuit Board

A printed circuit board (PCB) in the form of an Arduino shield [28] was constructed to hold the voltage regulator, displays, data storage module, some input devices, and connectors blocks (Fig. 4 and 5). All the necessary schematics to reproduce this PCB is readily available at the minimal request to the corresponding author.

3.2. Power supply

All the chosen electronics components use 5 volts to operate. A 12 V rechargeable sealed lead acid battery (one from the battery bank that powers the DCEM) was used connected to a power block in the PCB. From there, the voltage is regulated to 5V through a 7805 integral-circuit (IC) regulator [29] and filtered using a 10v 450 μF capacitor.

3.3. Sensors

Since the long term of the project is to reduce the contamination from fossil fuels, it is important to measure the power consumption of our load in terms of the fuel used, the electric energy consumed at any RPM and load conditions. In the following, the sensors employed are shown.

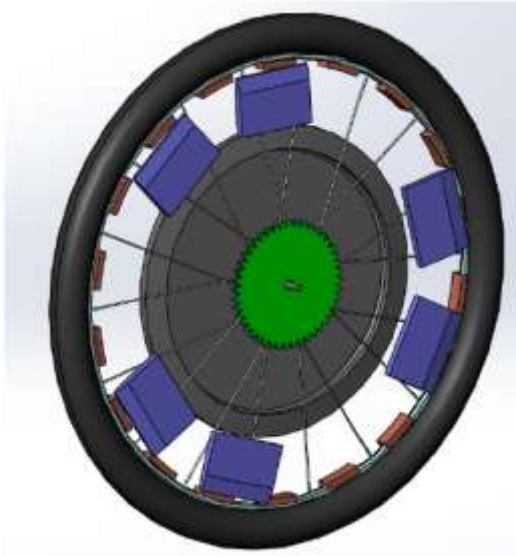

Figure 3. The load consists of the original wheel whose moment of inertia has been increased using a concentric weight plate and masses at the edge of the rim. The render shows only one gear of the multiple gear set.

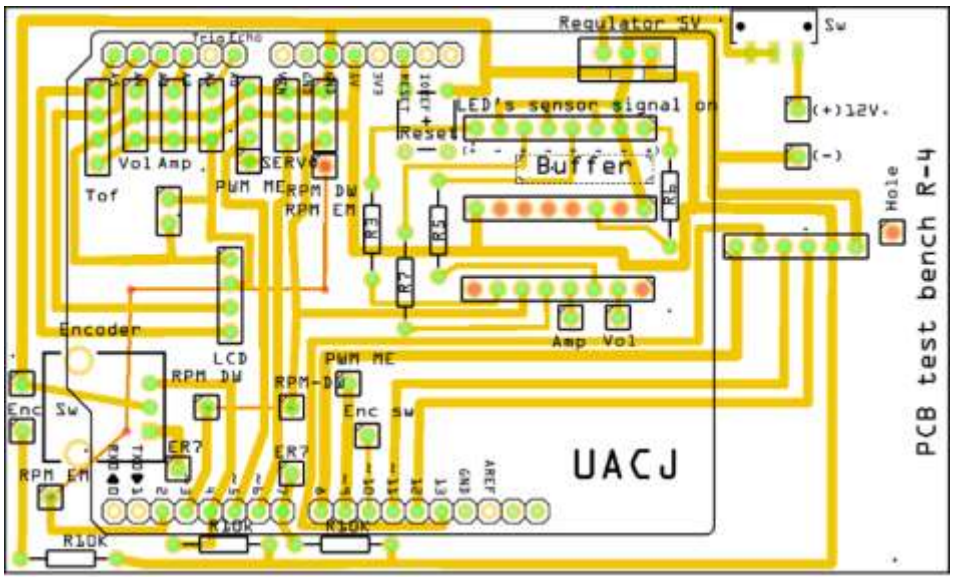

Figure 4. Arduino shield PCB interconnecting sensors, displays and actuators with the microprocessor.

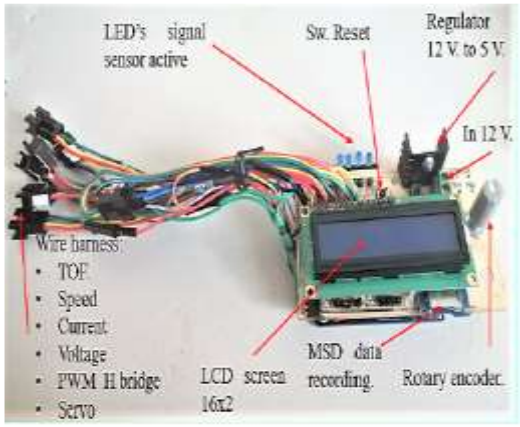

Figure 5. Arduino shield PCB interconnecting sensors, displays and actuators with the microprocessor.

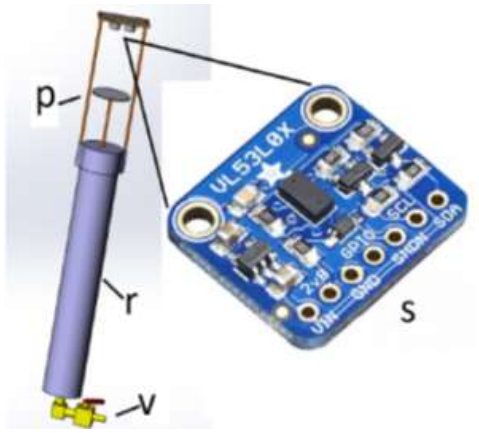

Figure 6. Sensor to measure fuel consumption using the VL53L0X module. A PCV reservoir (r) contains a float connected to a plate (p) through a dipstick. The VL53L0X emits a laser pulse to this plate, and it measures the TOF inferring the distance. This information is proportional to fuel amount in the reservoir.

3.3.1. Fuel Sensor

At the writing of this article, the authors did not find any sensor capable of measuring in the ml/min range, fuel safe and cheap. Therefore, fuel measuring device was constructed based on the VL53l0X sensor [30] in its module mode (Figure 6). This sensor uses the time of flight (TOF) concept to measure the distance that a light pulse travels from the sensor to an obstruction and, back. This sensor can be used up to 2 meters with +/- 1 mm accuracy. The proposed fuel sensor consists of a cylinder made from commercial PCV pipe of known internal area. The cylinder is mounted at the fuel tank height and fed with fuel from it through a hose. This configuration allows that the tank and the fuel inside the sensor share the same fuel level. Inside the PCV cylinder there is a fuel float connected to an external plate through a dipstick. The TOF sensor is placed at the top of a PCV cylinder pointing to this plate. The fuel metering is indirectly achieved by measuring the distance between the TOF sensor and this plate which is proportional to the fuel level inside the PCV cylinder. This information is sent to the micro-controller using the I2C protocol [31].

3.3.2. Current and Voltage

One important variable to consider in the investigation of hybrid engines is the power consumed by the DCEM. To do so, it is

necessary to know its operation voltage and current consumption. For current, a module based on the ACS7121 IC was used that delivers a voltage from 0 to 5V proportional to the measured current [32]. For voltage monitoring, a module that simply uses a voltage divider to map 0-25V in to 0-5V was employed. These output levels are easily read by the micro-controller on its analog input ports. Even that these cheap sensors come ready to use, it is always a good practice to compare their outputs with a calibrated meter and to software-compensate any discrepancies.

3.3.3. RPM

To measure the period of rotation and infer the RPM, an LED Photo-diode interruption sensor was used in its slotted module form. This sensor delivers a TTL logic signal when there is an object between the LED and the photodiode. This sensor was placed in the gear of the inertia wheel in such a way the gear tooth can interrupt the light path. By measuring the time between each light interruption, the RPM can be inferred as the revolution period inverse of the inertia load.

3.4. Data storage and displays

It is of importance to log all the possible information for post-processing and analysis. Also, is very helpful to watch the information flow in real-time. For these reasons, our PCB includes means of storage and information display.

3.4.1. SD Card

To record the data, a security card (SD) module was chosen that reads and records over a mini-SD card. This type of module is cheap and can be directly interfaced to the micro-controller through the SPI protocol [33].

3.4.2. LCD and LEDs

An 16X2 line LCD is placed in front of the PCB to display in real-time the most important data and to navigate through menus. Our display is not directly driven by the micro-controller; it uses a module based on the PCF8574 IC [34] that allows for the LCD to be operated through the I2C protocol using only 4 inputs, saving I/O ports for other uses.

At the beginning of a test run and with the use of a rotary encoder, the LCD allows to navigate through menus and select the type of experiment the user want to make. During the experiment, it displays basic information like the power consumed by the DCEM and the RPM. Even that all the data from the sensors is being recorded, PCB light emitting diodes (LED's) were included that allows to corroborate, in real-time, the proper functioning of the device. This is a quick method to check if the device is reading a signal from the sensors and/or to the actuators. The LEDs are indirectly driven by a CD4050BE IC working as a buffer [35], so the current drop from the LED's does not affect the sensor or micro-controller signals.

3.5. Actuators and Controls

With the aim of having consistent data, is desirable to automatically control the power delivered by the DCEM and the ICE. For the DCEM, the power control is achieved by regulating the input current, and for the ICE, by adjusting the amount of air/fuel (A/F) mixture entering the combustion chamber.

3.5.1. Current Regulator

To control the DCEM current, a module based on the BTS7960 IC [35] was used connected in parallel with the DCEM and the battery bank. This type of module is a H-bridge that allows to control the DCEM direction of rotation, freewheeling or stopping. The latter can be used to reconvert the kinetic energy of the load back into current to the batteries. The amount of current supplied to the DCEM from the battery is controlled by a square wave signal of constant amplitude and adjustable width supplied by the microcontroller. The amperage is proportional to the width of this square wave. This type of control is commonly known as pulse width modulation (PWM) [35].

3.5.2. The air/fuel control

The A/F control is achieved by controlling the throttle opening in the ICE carburetor. Originally, the throttle is cable operated, therefore a fixture was design and fabricated that allows to couple this cable to a servo motor. The servomotor is a type of electric motor that allows control over its angular position through a digital signal [36]. The fixture converts the angular position to linear displacement of the cable. In this way, the power delivered by the ICE can be controlled trough the micro-controller (figure 7).

3.5.3. Buttons and rotary encoder

The user inputs to the test bench are through push buttons and a rotary encoder [36] with a 20 steps/revolution. These allow to reset the system or move across menus displayed in the LCD. Also, in one of the operation modes, the rotary encoder allows to directly operate the servomotor to manually control the power delivered by the ICE. This is useful for warming the ICE or just to vary the engine RPM to verify its operation.

4. Operation and control algorithm

In this section, three operation examples for the test bench are presented as a basis for other operation routines depending on the specific research goals. A simplified and general version of the algorithm for these routines are given in the figure (8). For all the ICE modes below, it is necessary to perform the following procedure:

1. Open tank valve A to fill the fuel from the tank to the fuel sensor.
2. Turn on a main switch to power all the electronics and DCEM.
3. Select the starting engine option on the LCD and push the encoder button.
4. Activate the carburetor choke and manually start the engine. Once it starts, the throttle can be controlled using the rotary encoder. Deactivate the choke and warm up the ICE.
5. Using the rotary encoder, set the ICE to idle and press the button. The LCD will return to the main menu.
6. Select the desired routine.

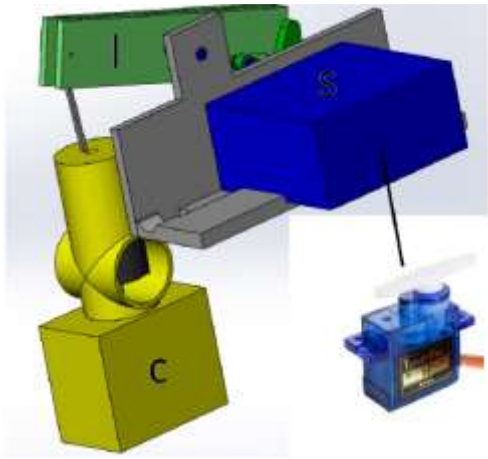

Figure 7. Electro-mechanical device to control the A/F mixture. It consists of a servo motor (S) coupled to a lever (L). At the other end of the lever, there is the throttle cable that operates the carburetor (C).

4.1. ICE engine dyno program

The engine dyno program simply commands the throttle actuator to go to its maximum value and record the revolution periods of the inertia wheel. With this information, the RPM´s as a function of time can be obtained and subsequently the angular acceleration to acquire the dynamical curve for torque and power from the ICE. The power and torque are calculated by:

$$\tau = I\frac{d\omega}{dt}, \qquad \textbf{(Eq. 3)}$$

$$P = \tau\omega, \qquad \textbf{(Eq. 4)}$$

where τ is the torque, P the power, I the moment of inertia, ω the rotational speed and the derivative dω/dt is finite difference approximated.

The run is manually stopped when the operator observes that the RPM are not changing. In a future code revision, a maximum RPM can be set to stop the acquisition run. The data is then transferred to a computer via the SD card for post processing.

4.2. ICE only routine.

In this routine, the micro controller sets the throttle to a constant value for a period. It displays the RPM on the LCD, and it saves the information on fuel consumption and revolution period. The simplified algorithm is

given in figure (8). This routine could be used to quantify the fuel consumption for a given RPM.

4.2.1. DCEM and ICE routine.
This routine is like the above, with the exception that the DCEM now is also supplying power. The fuel consumption, current, voltage, RPM are saved on the micro-SD card. This routine is a first attempt to investigate how much fuel can be saved using a DCEM in parallel.

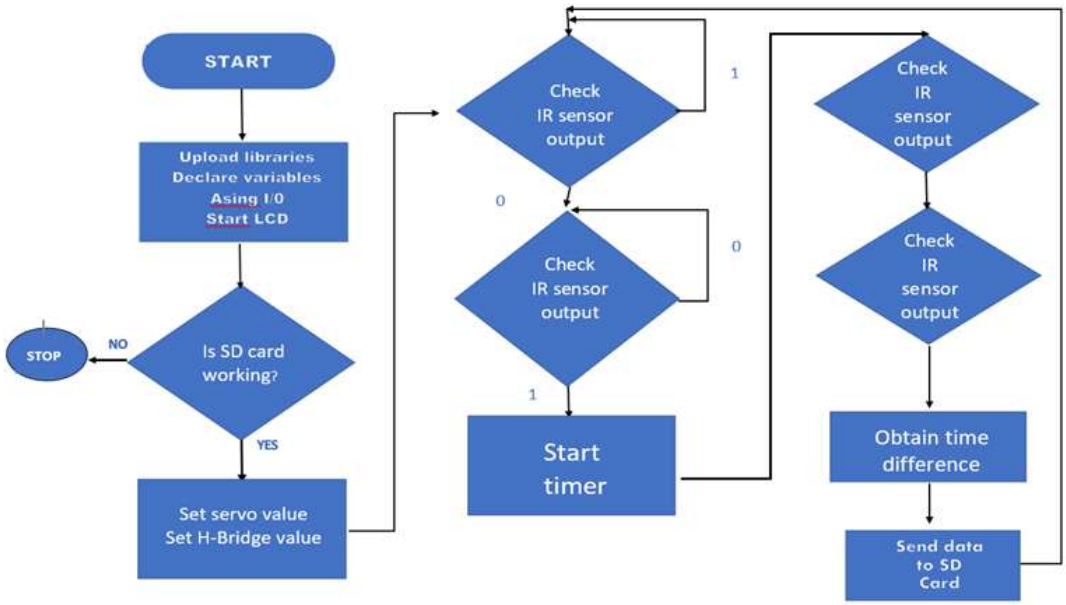

Figure 8. Simplified and general algorithm for testing. A) Dyno program: the servo is set to maximum and the DCEM control to zero. B) ICE only routine: the servo is set to a medium value and DCEM to zero. C) DCEM and ICE: both the servo and DCEM control are set to an intermediate value.

5. Results and analysis

It is desirable to represent the obtained data as a function of time. Since our system does not contain an external clock, a cumulative summing the revolution period data was opted to obtain the time parameter.
Even that the graphs below show one test, it is worth mentioning that the graphs obtained from several runs maintained the same, width, height, and shape within the maximum error propagation of the sensors and acquisitors accuracy, giving the confidence on the reliability of the device.

5.1. Dynamometer results
Figure (9) shows the raw data in revolutions per second. It can be observed that the data contains spikes that does not represent real information. These spikes are detected and removed by replacing them with an average of their neighbour points. Also, a moving average is applied to smooth out the curve for future calculations.

Figure 10 shows the dynamometer run result, where a peak power below 400 watts around 250 RPM can be observed. The total gear ratio from engine to load is 18:1, therefore the maximum power occurs in the engine at 4500 RPM which is typical for this type of ICEs. After 320 RPM, the figure also shows a fluctuating behavior due to the inclusion of the deceleration data in the torque and power calculation.

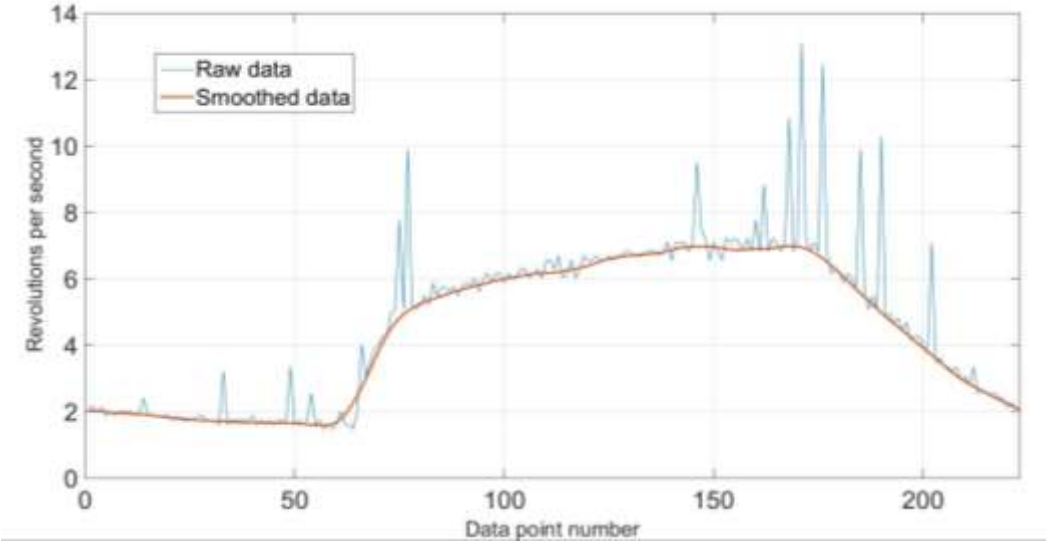

Figure 9. Raw and smoothed data from the infrared sensor. All the tests were performed at 27 °C, 1018 mb and 60% humidity.

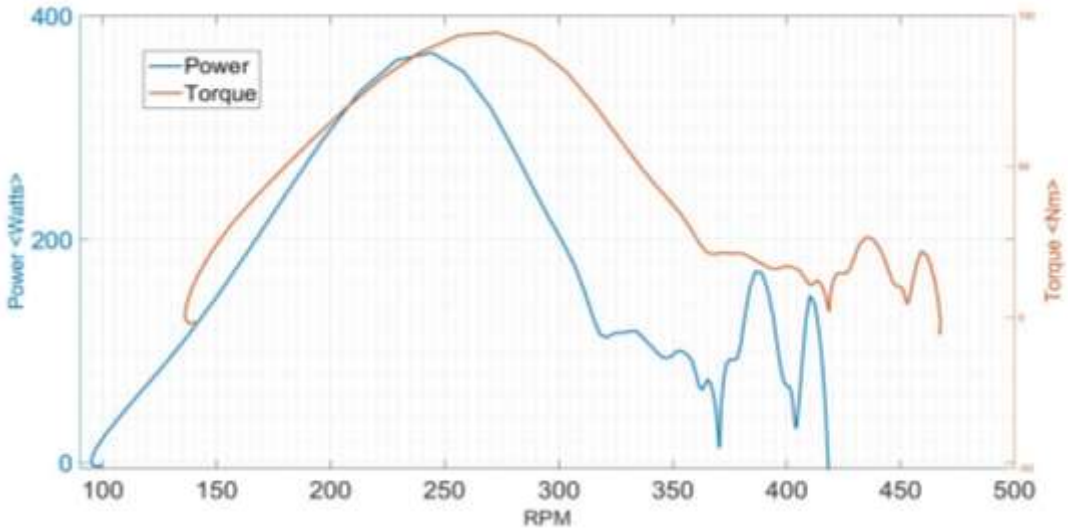

Figure 10. Torque and power vs RPM.

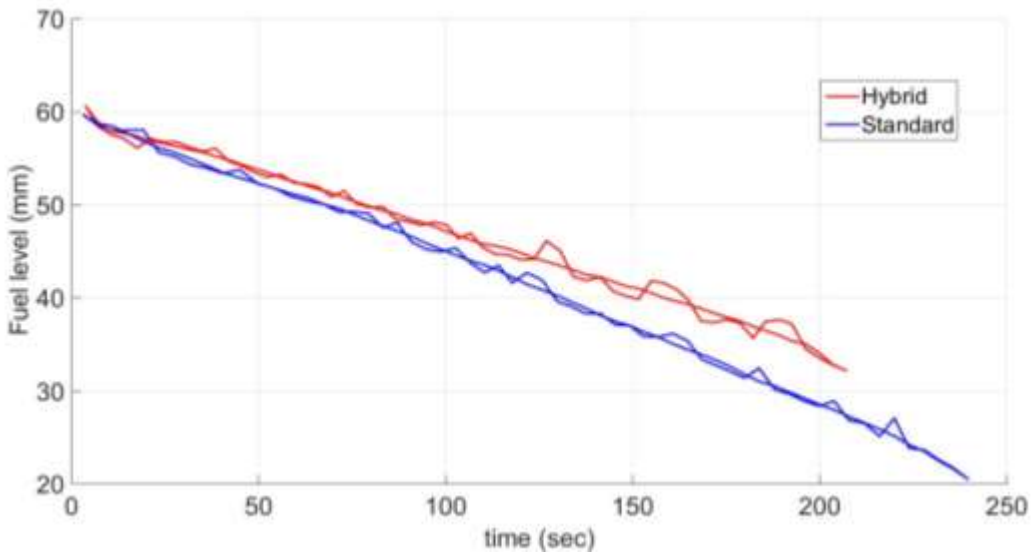

Figure 11. The figure shows the fuel consumption as a function of time with and without the use of the DCEM. The straight lines are moving averages showing the fuel saving rate for the hybrid case.

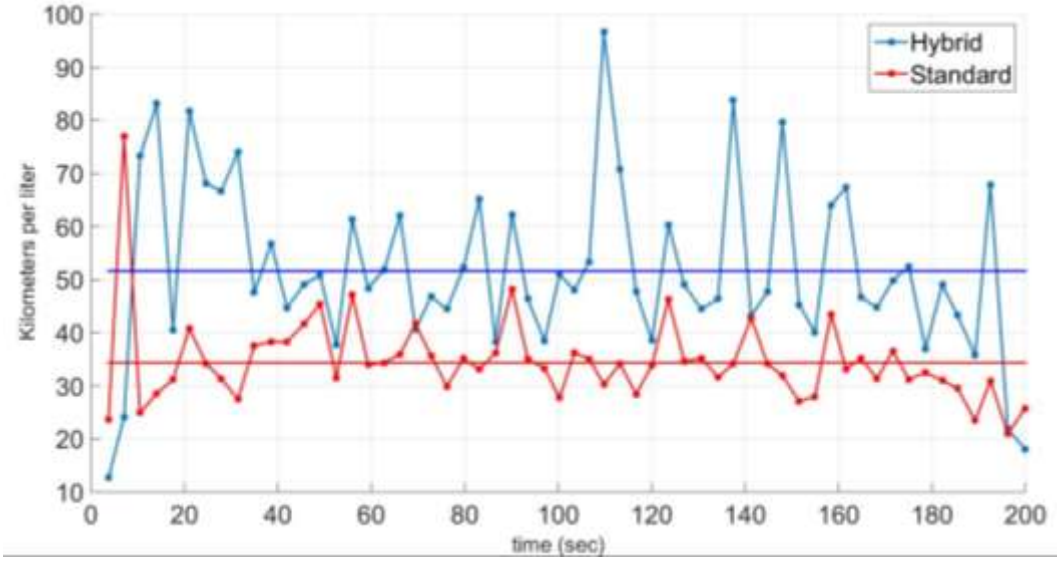

Figure 12. The graph is a time series of the kilometers per liter achieved with and without the aid of the DCEM. The flat lines are the average of each run.

5.2. ICE and DCEM routine

The graphs in figures 11 and 12 shows the fuel level and consumption (kilometers per liter) vs time for the ICE running at a constant speed.

Afterwards, the same test is done with the difference that now the DCEM is activated proportioning power to the load. The purpose of this simple experiment is to show the fuel sensor capabilities and to make first estimations of the fuel savings. In this case, it can be observed a consumption change from 34 to 51 kilometers per litter.

In a future work, this information will be correlated with the energy consumption of the DCEM, for different travel routines and conditions in order to calculate the payback period of converting an originally ICE vehicle into hybrid.

6. Conclusions and future work

The design and testing of a low-cost test bench for hybrid conversion research was presented. The device hardware is robust, versatile, and reliable: the load can be powered by three power sources; it can acquire RPM, fuel consumption, current and voltage and can control the DCEM and ICE power output. In addition, the device includes a very convenient system for displaying and recording data. The recorded data was consistent as several runs under similar conditions showed graphs of very similar height, width, and shape.

Because the system is based on the Arduino system, the programming can be done in a very accessible way: for instance, acceleration cycles of the ICE or DCEM control algorithms can be implemented directly. Moreover, the system general behaviour can be modified. For example, the user may decide to send the information directly to the computer (trough the USB) instead of saving it to the SD card. This can be easily programmed on the micro-controller.

All the above features allow to obtain first results about the algorithms and/or architecture used in converted hybrid vehicles for testing its performance under different conditions. Future work includes the addition of a device that allows to control the friction load. This could be done by adding a screw operated friction device, like the one used on stationary exercise bicycles. The screw could then be driven by a micro-controller-controlled stepper motor.

This device is suitable for academic purposes and/or new ideas proof of concept. In theory, all the results obtained can be linearly

extrapolated to larger vehicles as long the scale factors are acknowledged; but in order to confirm or publish any results, certified equipment is recommended. Finally, it's the authors desire that the information in this paper helps researchers and hobbyist to make region specific research in their developing countries.

7. References

1. Bayindir, K. Ç., Gözüküçük, M. A., & Teke, A. (2011*)." A* comprehensive overview of hybrid electric vehicle: Powertrain configurations, powertrain control techniques and electronic control units". *Energy conversion and Management, 52*(2), 1305-1313. https://doi.org/10.1016/j.enconman.2010.09.028

2. Shen, C., Shan, P., & Gao, T. (2011). "A comprehensive overview of hybrid electric vehicles". *International Journal of Vehicular Technology*, *2011*. doi:10.1155/2011/571683.

3. Andwari, A. M., Pesiridis, A., Rajoo, S., Martinez-Botas, R., & Esfahanian, V. (2017). "A review of Battery Electric Vehicle technology and readiness levels". *Renewable and Sustainable Energy Reviews*, 78, 414-430. DOI: 10.1016/j.rser.2017.03.138.

4. Hitha, P., Sosale, S. S., Sushmitha, S., & Rekha, K. R. (2017). "Performance analysis of various-4-wheelers with IC engines for hybridization". *International Journal of Advance Research, Ideas, and Innovations in Technology*, *3*(3), 1322-1327.

5. Teixeira, A. C. R., & Sodré, J. R. (2018). "Impacts of replacement of engine powered vehicles by electric vehicles on energy consumption and CO2 emissions". *Transportation Research Part D: Transport and Environment,* 59,375-384. https://doi.org/10.1016/j.trd.2018.01.004.

6. Moore, W. H. (1978). *U.S. Patent No. 4,090,577*. Washington, DC: U.S. Patent and Trademark Office.

7. Amjad, S., Neelakrishnan, S., & Rudramoorthy, R. (2010). "Review of design considerations and technological challenges for successful development and deployment of plug-in hybrid electric vehicles". *Renewable and Sustainable Energy Reviews*, 14(3),1104-1110. https://doi.org/10.1016/j.rser.2009.11.001

8. Burke, A. F. (2007). "Batteries and ultracapacitors for electric, hybrid, and fuel cell vehicles". *Proceedings of the IEEE*, *95*(4), 806-820. DOI: 10.1109/JPROC.2007.892490.

9. Guanetti, J., Formentin, S., & Savaresi, S. M. (2014). "Total cost minimization for next generation hybrid electric vehicles". *IFAC Proceedings*, Volumes, *47*(3), 4819-4824.

10. Farina, S., Firdaus, R. N., Azhar, F., Azri, M., Ahmad, M. S., Suhairi, R., & Sutikno, T. (2018). "Design and Analysis of In-Wheel Double Stator Slotted Rotor BLDC Motor for Electric Bicycle Application". *International Journal of Power Electronics and Drive Systems*, 9(1), 457. DOI: 10.11591/ijpeds. v9n1

11. Guan, Y., Zhu, Z. Q., Afinowi, I. A., Mipo, J. C., & Farah, P. (2014, October). "Comparison between induction machine and interior permanent magnet machine for electric vehicle application". In *2014 17th International Conference on Electrical Machines and Systems*

(ICEMS) (pp. 144-150). IEEE. DOI: 10.1109/ICEMS.2014.7013454

12. Tribioli, L., Barbieri, M., Capata, R., Sciubba, E., Jannelli, E., & Bella, G. (2014). "A real time energy management strategy for plug-in hybrid electric vehicles based on optimal control theory". *Energy Procedia*, *45*, 949-958.

13. Cao, J., & Xiong, R. (2017). "Reinforcement learning-based real-time energy management for plug-in hybrid electric vehicle with hybrid energy storage system". *Energy Procedia*, *142*, 1896-1901.

14. Capasso, C., Lauria, D., & Veneri, O. (2017). "Optimal control strategy of ultra-capacitors in hybrid energy storage system for electric vehicles". *Energy Procedia*, *142*, 1914-1919.

15. Cao, J., & Emadi, A. (2011). "A new battery/ultracapacitor hybrid energy storage system for electric, hybrid, and plug-in hybrid electric vehicles". *IEEE Transactions on power electronics*, *27*(1), 122-132.

16. Naseri, F., Farjah, E., & Ghanbari, T. (2016). An efficient regenerative braking system based on battery/supercapacitor for electric, hybrid, and plug-in hybrid electric vehicles with BLDC motor". *IEEE Transactions on Vehicular Technology*, *66*(5), 3724-3738. DOI: 10.1109/TVT.2016.2611655

17. 18Qiu, C., Wang, G., Meng, M., & Shen, Y. (2018)." A novel control strategy of regenerative braking system for electric vehicles under safety critical driving situations". *Energy*, *149*, 329-340. https://doi.org/10.1016/j.energy.2018.02.046

18. Palmer, K., Tate, J. E., Wadud, Z., & Nellthorp, J. (2018). "Total cost of ownership and market share for hybrid and electric vehicles in the UK, US, and Japan". *Applied energy*, *209*, 108-119. https://doi.org/10.1016/j.apenergy.2017.10.089

19. Ehsani, M., Gao, Y., & Miller, J. M. (2007). "Hybrid electric vehicles: Architecture and motor drives". *Proceedings of the IEEE*, *95*(4), 719-728. DOI: 10.1109/JPROC.2007.892492

20. Silvaş, E., Hofman, T., & Steinbuch, M. (2012). „Review of optimal design strategies for hybrid electric vehicles". *IFAC Proceedings Volumes*, *45*(30), 57-64.

21. Hui, Z., Cheng, L., & Guojiang, Z. (2008, September)." Design of a versatile test bench for hybrid electric vehicles". In *2008 IEEE Vehicle Power and Propulsion Conference* (pp. 1-4). IEEE.

22. Salah, M., Abu Mallouh, M., Youssef, M., Abdelhafez, E., Hamdan, M., & Surgenor, B. (2017). "Hybrid vehicular fuel cell/battery powertrain test bench: design, construction, and performance testing". *Transactions of the Institute of Measurement and Control*, *39*(9), 1431-1440.doi:10.1177/0142331216642835.

23. Fajri, P., Ferdowsi, M., Lotfi, N., & Landers, R. (2016). „Development of an educational small-scale hybrid electric vehicle (HEV) setup". *IEEE Intelligent Transportation Systems Magazine*, *8*(2), 8-21. DOI: 10.1109/MITS.2015.2505739

24. Arduino.cc. Arduino Shield, unkown. Online accessed 08-24-2020.

25. Coveñas, J. L. (2014). *Diseño mecánico de un dinamómetro vehicular portátil para determinar la potencia de automóviles Rally de tracción simple*. Pontificia Universidad Católica del Perú.

26. Gallego, R. S., & Cerio, C. D. de. (2012). *Diseño mecánico de un banco de pruebas inercial para motocicletas*. Universidad publica de Navarra.

27. Montaluisa, G. (2007). *Diseño de un dinamómetro inercial y construcción de un modelo a escala*. Escuala politecnica Nacional. Retrieved from http://bibdigital.epn.edu.ec/handle/15000/88

28. Instrument, T. LM340, LM340A and LM7805 Family Wide VIN 1.5-A Fixed Voltage Regulators, 2016. [Online; accessed 02-September-2020].

29. St.co. VL530X, 2018. Online accessed 09-02-2020.

30. Robots didácticos. I2C, 2018. Online, accessed 02-September -2020.

31. Microsystems, A. ACS712: Fully Integrated, Hall-Effect-Based Linear Current Sensor IC with 2.1 kVRMS Voltage Isolation and a Low-Resistance Current Conductor, Unknown. [Online; accessed 02-September-2020].

32. Peripheral, T. D. S. (2001). Reference Guide. *Texas Instruments Literature Number SPRU109D*.

33. Instrument, T. PCF8574 Remote 8-Bit I/O Expander for I2C Bus, 2015. [Online; accessed 02-September-2020].

34. Instrument, T. CD4049UB and CD4050B CMOS Hex Inverting Buffer and Converter, 2020. [Online; accessed 02-September-2020].

35. Wang, M., & Jiang, Z. (2009, November). „The Design and Comparison of DC Motor Drive Circuit in Smart Car Competition". In *2009 IEEE International Conference on Intelligent Computing and Intelligent Systems* (Vol. 2, pp. 325-328). IEEE.

36. Chen, P., Jung, I. W., Walko, D. A., Li, Z., Gao, Y., Shenoy, G. K., & Wang, J. (2019). ltrafast photonic micro-systems to manipulate hard X-rays at 300 picoseconds". *Nature communications*, *10*(1), 1-9.

8. **Appendix**

Table of principal characteristics of sensors and actuators employed in the test bench.

Sensor/Actuator	**Use in the test bench**	**Principal Characteristics**
Servo MG995	Carburetor throttle control	4.8-6.0 Volts; 8.5 - 10.0 kg'cm; 120 degrees
Photo-diode interruption sensor	Load RPM	Light emission interference in an 11 mm slotted module, it uses a LM393 comparator integrated circuit to send a light off-on signal.
BTS7960 High power H bridge module	Current control for the DCEM	27 V, 43 ampere max capacity
ACS7121 IC Module	Current sensor	20 A max capacity, delivers a voltage from 0 to 5V proportional to the current.
Voltage divider	Voltage sensor	Voltage divider to map the DCEM voltage into 0 to 5V
Vl53l0xv TOF sensor module	Fuel tank gasoline level sensor	I2C signal interpreted as distance in mm
LCD 16X2	Test bench interface	I2C two lines 16 columns
Micro-SD Card Adapter	Data recording	5V or 3.3 V, Communication standard by SPI interface protocol with Arduino IDE, it supports micro-SD card (<=2G), micro SDHC card (<=32G) (high-speed card)
LM7805 integrated-circuit	Electronics voltage regulator	5-volt regulator, 1 ampere maximum current
Buffer 4050	Buffer for LED signals	6-ch, 3-V to 18-V